Inulin reduces *Ralstonia* invasion by promoting cooperation between *Lysinibacillus sphaericus* and *Pseudoarthrobacter* spp.

Tao Yan[1, #], Ying Guan[1, #], Xinlan Mei[1], Ziru Zhang[1], Tianxiang Zhu[1], Yang Gao[1], Yangchun Xu[1], Qirong Shen[1], Zhong Wei[1], Tianjie Yang[1, *]

[1] Key Lab of Organic-based Fertilizers of China, Jiangsu Provincial Key Lab of Solid Organic Waste Utilization, Jiangsu Collaborative Innovation Center of Solid Organic Wastes, Educational Ministry Engineering Center of Resource-saving fertilizers, Nanjing Agricultural University, Nanjing, Jiangsu 210095, China

* Correspondence: tjyang@njau.edu.cn

# These authors contributed equally

Abstract

In field production, beneficial microbial agents are typically applied along with key resources that beneficial microbes prefer to utilize. This practice aims to help the beneficial microbes colonize the field and exert their disease resistance functions. However, the mechanisms by which these key resources influence the colonization and disease resistance effects of beneficial microbes remain unknown. In this study, we found that inulin can enhance the growth capacity of *Lysinibacillus sphaericus* HR92 and its ability to inhibit *Ralstonia solanacearum*. Further investigation revealed that inulin can enhance strain HR92's flagellar assembly, bacterial chemotaxis, fatty acid metabolism, and siderophore synthesis capabilities, ultimately improving strain HR92's effectiveness in controlling bacterial wilt. Moreover, adding inulin to the soil can enrich *Pseudarthrobacter* strains. This genus enhances the expression of genes involved in the synthesis of the antibacterial substance HR92, and competes for nutrients with *Ralstonia solanacearum*, thereby further inhibiting the occurrence of bacterial wilt disease. Additionally, the combination of inulin and *Pseudarthrobacter* strains upregulates the valine and leucine pathway genes in strain HR92. These genes play a crucial role in the synthesis of surfactin and the antimicrobial VOC 3-methyl-1-butanol. We have demonstrated that the addition of key resources not

only enhances the control efficacy of beneficial bacteria against soil-borne diseases but also enriches the “helpers” of beneficial bacteria in soil.

Importance

Ralstonia solanacearum is a plant pathogen that can cause bacterial wilt in several important crops. Given the limitations of beneficial bacterial inoculation, we propose a strategy to enhance the biocontrol efficacy of beneficial microorganisms by utilizing key resources. In this study, we demonstrate that key resources inulin can improve the biological control effects of beneficial bacteria, thereby maintaining plant health. Furthermore, we found that increasing the concentration of inulin altered the diversity of the rhizosphere microbiota and specifically enriched the abundance of *Pseudarthrobacter*, which compete with pathogens for nutrients on one hand and, on the other hand, synergize with inulin to enhance the biocontrol efficacy of the beneficial biacterium HR92. Together, our study reveals that key resources can enhance the biocontrol efficacy of beneficial bacteria and enrich potential beneficial bacteria in resident microbial communities, further reducing tomato diseases.

Keywords: Tomato bacterial wilt, *Ralstonia solanacearum*, rhizosphere, inulin, *Lysinibacillus sphaericus*

Introduction

Soil-borne plant pathogens cause major economic losses to agricultural production due to lack of efficient control methods (1–5). In recent years, researchers have increasingly explored the use of biological control methods, which are ecologically friendly and exhibit specificity in pathogen suppression (6–9). Beneficial microbes can prevent pathogenic invasion of plant root systems through various mechanisms, they can secrete antagonistic substances that directly inhibit the growth of pathogens or their "helpers" (10), preventing colonization or invasion of plant roots. Some beneficial bacteria compete with pathogens for rhizosphere resources, thereby suppressing pathogen growth through nutrient competition. Moreover, introduced beneficial microbes can stimulate soil native resident microbiomes (11), engaging in metabolic interactions that fortify the rhizosphere, creating a more resilient barrier that pathogens find difficult to breach (10, 12–15). Studies have shown that *Lysinibacillus sphaericus* is an effective biocontrol agent against bacterial wilt in tomatoes (16–19). Specifically, *L. sphaericus* inhibits the growth of *R. solanacearum* through the secretion of volatile organic compounds (VOCs) such as dicarboxylic esters and 3-methyl-1-butanol (20), as well as cyclic lipopeptides like surfactin and bacitracin (21–23).

Due to the limited availability of nutrients in the rhizosphere and the complex conditions of the field environment (24, 25), the inoculated beneficial bacteria often lack a competitive edge over soil native resident microbiomes, preventing them from efficiently colonizing the rhizosphere and exhibiting their disease-suppressive functions (26–28). Recent studies have proposed providing nutritional carriers for inoculated beneficial bacteria to enhance their biocontrol efficacy in the rhizosphere (29–34). For instance, adding organic fertilizers, biochar, or amino acid-based fertilizers along with the beneficial microbes has been shown to improve their survival in the rhizosphere. However, these organic carriers are generally utilized by a wide range of soil microorganisms, lacking specificity, and cannot be exclusively exploited by beneficial bacteria. In recent years, research in the field of gut

microbiota has suggested adding resources preferentially utilized by beneficial bacteria along with their introduction to target and enhance their colonization in the gut (35, 36). Due to the analogous roles of the rhizosphere and the gut in host immunity and ecological function, we hypothesize that the application of targeted resources capable of selectively enhancing the colonization efficiency of beneficial bacteria in the rhizosphere will promote their stable establishment in the root environment (37–39), ultimately improving their biocontrol performance. Soil microorganisms in the rhizosphere are often strongly influenced by plant root exudates, with sugars in these exudates playing a crucial role in recruiting beneficial bacteria and maintaining plant health (40–42). Thus, we focused on soluble sugars from root exudates to identify a compound capable of selectively enhancing the colonization capacity of *Lysinibacillus sphaericus*. Through this approach, we aim to explore how such a resource influences the biocontrol potential of beneficial bacteria within the complex rhizosphere environment.

Unlocking the potential of specific resources to enhance the targeted colonization of beneficial bacteria in the rhizosphere, while understanding their effects on soil native microbial communities, is crucial for managing soil-borne diseases in agricultural production. We utilized *L. sphaericus* HR92 along with inulin, which has been shown to boost both the growth and antibacterial activity of strain HR92. By inoculating the beneficial bacteria and varying concentrations of inulin to the tomato roots, we observed the colonization potential of strain HR92 and its impact on the assembly of bacterial communities in the tomato rhizosphere. Our findings reveal that inulin not only directly enhances strain HR92 colonization and disease suppression capabilities but also enriches specific soil native resident microbiomes. These native microbes, on one hand, exhibit inhibitory effects on pathogens and, on the other, enhance the disease resistance of beneficial bacteria. Finally, we used transcriptomics to determine the influence of inulin and native soil microbes on strain HR92.

104 ## Materials and methods

105 ### Strains and growth conditions

106 The plant pathogen used in this study was *Ralstonia solanacearum* QL-Rs1115
107 (GenBank: GU390462) (43). The beneficial bacterium used in this study was
108 *Lysinibacillus sphaericus* HR92 (GenBank: JF700465.1) (19). The strain was routinely
109 grown in nutrient broth medium at 30°C with shaking at 170 rpm (10.0 g glucose L^{-1};
110 5.0 g peptone L^{-1}, 0.5 g yeast extract L^{-1}, and 3.0 g beef extract L^{-1}, pH 7.0).
111 In *vitro* co-culture experiments, we utilized strain *Ralstonia solanacearum* QL-Rs1115,
112 which was tagged with the pYC12-mCherry plasmid (excitation light: 587 nm,
113 absorption light: 610 nm) (14), and strain HR92, which carries green fluorescence
114 (excitation light: 488 nm, absorption light: 510 nm).

115 ### Greenhouse experiment setup and sample collection

116 Surface-sterilized tomato seeds (Solan*um lycopersicum,* cultivar "Hong'ai") were
117 germinated on water-agar plates for 3 days before sowing into 54-well trays filled
118 with growth substrate (50 g substrate per well; commercially available from
119 Jiangsu-Xingnong Substrate Technology Co., Ltd). At the three-leaf stage (17 days
120 after sowing), a subset of tomato plants of similar size was selected and transplanted
121 into nine-cell plant trays containing either natural or sterilized soil (200 g per cell).
122 Seedling were grown under controlled greenhouse conditions (25-30°C, 16/8 h
123 day/night cycle, 200 μmol m^{-2} s^{-1} light density, and 70% relative humidity).
124 Seven days after transplantation, strain HR92 and inulin were inoculated into the
125 rhizosphere soil of each plant. The final density of strain HR92 was 1×10^8 CFU g^{-1}
126 soil. The final concentration of inulin was adjusted according to each treatment.
127 Seven days after inoculating strain HR92 and inulin, *R. solanacearum* was inoculated
128 into the rhizosphere soil of each plant at a final density of 1×10^6 CFU g^{-1} soil.
129 The experiment comprised four treatments: (i) Only pathogen: plants inoculated only
130 with *R. solanacearum* (RS); (ii) HR92: beneficial bacteria HR92 introduced one week
131 prior to inoculation with *R. solanacearum*; (iii) HR92 + 0.1% wv^{-1} inulin: strain HR92
132 and inulin (1 g kg^{-1} soil) introduced one week prior to inoculation with *R.*

133 *solanacearum*; (iv) HR92 + 0.3% wv^{-1} inulin: strain HR92 and inulin (3 g kg^{-1} soil)
134 introduced one week prior to inoculation with *R. solanacearum* (Fig. S1). Each
135 treatment had four biological replicates, with each replicate consisting of five
136 individual tomato plants, resulting in a total of 80 plants (20 plants per treatment).
137 Tomato plants regularly watered with sterile water, and plant positions were
138 randomized within treatments every two days.
139 Seven days after inoculation with *R. solanacearum*, the tomato plants began to
140 exhibit disease symptoms. Once the disease reached a stable state, the incidence of
141 disease was recorded, and soil samples from the rhizosphere of both healthy and
142 diseased plants were collected and stored at -80°C. Disease severity (DS) was
143 quantified using a disease index (DI) ranging from **0** to **4** (**0**, no signs of wilting; **1**,
144 1%–25% lead area wilted; **2**, 26%–50% leaf area wilted; **3**, 51%–75% leaf area wilted;
145 and **4**, 76%–100% leaf area wilted), and was calculated using the formula: DS = ∑
146 (number of diseased plants with given index × DI)/ (total number of plants infected ×
147 highest DI) (44).
148 **DNA extraction and 16S rRNA gene amplicon sequencing**
149 Genomic DNA was extracted from 0.5 g of soil using the PowerSoil® DNA Isolation Kit
150 (MoBio, Carlsbad, CA, USA) following the manufacturer's instructions. The purity and
151 concentration of DNA were determined using a NanoDrop ND-1000
152 spectrophotometer (Thermo Fisher Scientific, Carlsbad, CA, USA) and a Qubit 2.0
153 fluorometer (Thermo Fisher Scientific).
154 The V4 region of the bacterial 16S rRNA gene was amplified with primers 563F and
155 802R (Table S3) (45). A two-step dual indexing strategy for Illumina MiSeq (Illumina,
156 San Diego, CA, USA) sequencing was employed. The PCR thermocycler program
157 included an initial denaturation temperature of 95°C for 2 min, then 25 cycles of 95°C
158 for 30 s, 55°C for 30 s, and 72°C for 30 s, and a final elongation step of 72°C for 5 min.
159 The PCR amplification was confirmed by gel electrophoresis on 2% agarose gels. PCR
160 products were purified using AxyPrep PCR Clean-up Kit (Axygen Biosciences, CA, USA).
161 The following library construction and Illumina MiSeq sequencing (2 × 300 bp) were

162 performed by Shanghai Biozeron Biological Technology (Shanghai, China).

163 Raw amplicon reads were processed using the DADA2 pipeline v.1.14.1 (46). In brief,
164 reads were quality checked and primers were removed using trimLeft in the filter
165 AndTrim function. According to the sequence quality, the 16S rRNA gene reads were
166 filtered using default parameters (confidence level at 80 %). Chimeras were removed
167 after merging denoised pair-end sequences. Each unique amplicon sequence variant
168 (ASV) was assigned to taxa according to SILVA database v.138.1 (47) for the 16S rRNA
169 gene. For bacteria, non-bacterial ASVs including chloroplasts and mitochondrial reads
170 were removed.

171 **Real-time quantitative PCR analysis**

172 Quantification of strain HR92 (19) and *R. solanacearum* (48) was performed by qPCR
173 using the qTOWER Real-Time PCR system (Analytik jena, Jena, Germany). The specific
174 primers utilized are listed in Table S3. Twenty-microliter reactions were containing 10
175 μL of 2X TB Green Premix Ex Taq (TaKaRa, Beijing, China), 2 μL of DNA, 0.8 μL of each
176 primer (10 μM), 0.4 μL of ROX Reference Dye (TaKaRa, Beijing, China) and 6 μL of
177 Nuclease-free water. Thermal cycling conditions were as follows: 95°C for 3 min,
178 followed by 40 cycles of 95°C for 30 s, 50°C for 30 s, and 72°C for 30 s. Standard
179 curves were used to calculate the gene copy numbers of the target group for each
180 reaction. Each sample was run in triplicate, and results were expressed as log10
181 values of the gene copy numbers per gram of soil.

182 **Screening of rhizosphere bacteria**

183 Bacteria were isolated from the rhizosphere soil of five healthy tomato plants by
184 suspending 1 g of soil in 9 ml of sterile distilled water, followed by vigorous vortexing
185 and serial dilution. One hundred microliters of serial dilutions (10^{-4}-10^{-7}) were plated
186 onto 1/3 TSA agar plates (tryptone 5 g L^{-1}, soy peptone 1.65 g L^{-1}, NaCl 1.65 g L^{-1} and
187 agar 15 g L^{-1}). Plates were incubated at 28°C for 5 days, after which 32 single colonies
188 were selected from each soil sample based on bacterial morphology.

189 The isolates were identified based on 16S rRNA gene sequence using universal
190 primers 27F and 1492R (Table S3) (49). PCR products were sequenced by Sangon
191 Biotech (Shanghai Co., Ltd, China). 16S rRNA gene sequencing results were blasted

192 against the NCBI database for homologous sequences.

193 **Carbon resource utilization patterns of the bacterial isolates**

194 The resource utilization patterns of four bacterial isolates were assessed across 74
195 distinct monocarbon resources (Table S2), including amino acids, organic acids, and
196 sugars commonly found in tomato root exudates. Bacterial isolates were grown
197 overnight in TSB medium (tryptone 15 g L^{-1}, soy peptone 5 g L^{-1} and NaCl 5 g L^{-1}) at
198 30°C with shaking at 170 rpm. Cells were washed three times with 0.85% wv^{-1} NaCl
199 and resuspended to an OD_{600} of 0.5. Then, 5 µl of each suspension was added to a
200 384-well microtiter plate containing 40 µl of OS minimal medium (50) supplemented
201 with 5 µl of 1 mM of different carbon sources. Plates were incubated at 30°C with
202 agitation at 170 rpm, and bacteria growth was measured after 48 h using a
203 SpectraMax M5 spectrophotometer (Molecular Devices, Sunnyvale, CA, USA).

204 The 48-hour biomass (OD_{600}) of each bacterial strain cultured in water was used as a
205 control. T-tests were conducted to compare the biomass of bacteria under each
206 resource condition with the biomass under the control condition. A significance level
207 of $p < 0.05$ indicated that the bacteria could utilize the respective resource.
208 Utilization efficiency was calculated using the formula: (biomass under resource
209 condition - control)/ control. Utilization efficiency was categorized into different
210 levels: below 20% was marked as *, 20%-40% as **, 40%-60% as ***, and above 60%
211 as ****.

212 **Effect of inulin on bacterial growth**

213 The bacterial strains HR92, P265 (*Pseudarthrobacter siccitolerans*), and P397
214 (*Pseudarthrobacter oxydans*), and *R. solanacearum* QL-Rs1115 were grown overnight
215 in NB medium at 30°C with shaking at 170 rpm. Cells were washed three times with
216 0.85% wv^{-1} NaCl and resuspended to an OD_{600} of 0.5. Then, 2 µL of each suspension
217 was added to a 96-well microtiter plate containing 178 µL of NB medium and 20 µL
218 of 3% inulin (w/v). Plates were incubated at 30°C with agitation at 170 rpm, and
219 bacteria growth (OD_{600}) was measured after 48h using a SpectraMax M5
220 spectrophotometer (Molecular Devices, Sunnyvale, CA, USA). After measurement,
221 the bacterial suspension was transferred to a 96-well filter membrane plate and

222 centrifuged at 3000 rpm for 15 minutes to collect the supernatant (supernatant 1).

223 **Impact of Inulin on *R. solanacearum* suppression by bacterial supernatant**

224 Two microliters of bacterial solution (OD_{600} = 0.5) were added to a 96-well microtiter
225 plate containing 178 µl of NB medium and 20 µl of supernatant 1. Plates were
226 incubated at 30°C with agitation at 170 rpm, and bacteria growth (OD_{600}) was
227 measured after 48 h using a SpectraMax M5 spectrophotometer (Molecular Devices,
228 Sunnyvale, CA, USA). The inhibition ability of strain HR92 or *Pseudoarthrobacter*
229 strains against *R. solanacearum* was analyzed by examining the biomass of *R.*
230 *solanacearum.*

231 **Impact of inulin on *R. solanacearum* suppression when coculturing with**
232 **rhizosphere bacteria**

233 2 µL of bacterial solution (OD_{600} = 0.5) of strain HR92, P265 or P397 were individually
234 added with 2 µL of *R. solanacearum*-RFP to a 96-well microtiter plate containing 176
235 µl of NB medium and 20 µl of 3% inulin (w/v). Plates were incubated at 30°C with
236 agitation at 170 rpm. After 48 h, the OD_{600} value and red fluorescence value were
237 measured. We use red fluorescence (RFU) and OD600 to calculate the relative
238 abundance of *R. solanacearum* (51). Afterwards, we compared the relative
239 abundance of *R. solanacearum* in different treatments to demonstrate the inhibitory
240 effect of rhizosphere bacteria on pathogens during co-culture: $\log_{10}$ (RFU/OD_{600}
241 value).

242 **Effect of *Pseudoarthrobacter* spp. and inulin on the ability of strain HR92 to inhibit**
243 ***R. solanacearum***

244 This experiment followed a three-step workflow that was similar to previous
245 inhibition assays. Initially, 2 µL of bacterial suspension (OD_{600} = 0.5) of strain P265 or
246 P397 were incubated in 178 µL of NB medium with 20 µL of 3% inulin (w/v) at 30°C
247 with agitation at 170 rpm for 48 h. The resulting bacterial suspension was transferred
248 to a 96-well filter membrane plate and centrifuged at 3000 rpm for 15 min to collect
249 the supernatant (supernatant 2-1). Next, 2 µL of bacterial suspension (OD_{600} = 0.5) of
250 strain HR92 was incubated with 178 µL of NB medium and 20 µL of supernatant 2-1
251 under same conditions for 48 h. The bacterial suspension was then centrifuged, and

252 the supernatant (supernatant 2-2) was collected. Finally, 2 μL of *R. solanacearum*
253 suspension (OD_{600} = 0.5) was incubated with 178 μL of NB medium and 20 μL of
254 supernatant 2-2 at 30°C with agitation at 170 rpm for 48 h. Bacterial growth (OD_{600})
255 was measured using a SpectraMax M5 spectrophotometer (Molecular Devices,
256 Sunnyvale, CA, USA). The effect of *Pseudoarthrobacter* spp. and inulin on the ability
257 of strain HR92 to inhibit *R. solanacearum* was analyzed by examining the biomass of
258 *R. solanacearum*.

259 **Effect of strain HR92 on the ability of *Pseudoarthrobacter* spp. to inhibit *R.***
260 ***solanacearum***

261 This experiment followed a three-step workflow similarly to the previous inhibition
262 assays. Initially, 2 μL of strain HR92 suspension (OD_{600} = 0.5) were incubated with 178
263 μL of NB medium and 20 μL of 3% inulin (w/v) at 30°C with agitation at 170 rpm for
264 48 h, and the supernatant (supernatant 3-1) was collected after centrifugation. Next,
265 2 μL of *Pseudoarthrobacter* strains (strain P265 or P397) suspension (OD_{600} = 0.5) was
266 incubated with 178 μL of NB medium and 20 μL of supernatant 3-1 under similar
267 conditions for 48 h, followed by centrifugation to collect the supernatant
268 (supernatant 3-2). Finally, 2 μL of *R. solanacearum* suspension (OD_{600} = 0.5) was
269 incubated with 178 μL of NB medium and 20 μL of supernatant 3-2 at 30°C with
270 agitation at 170 rpm for 48 h, and bacterial growth (OD_{600}) was measured using a
271 SpectraMax M5 spectrophotometer (Molecular Devices, Sunnyvale, CA, USA). The
272 effect of strain HR92 on the ability of *Pseudoarthrobacter* spp. to inhibit *R.*
273 *solanacearum* was analyzed by examining the biomass of *R. solanacearum*.

274 **Effect of 3-methyl-1-butanol on the growth of *R. solanacearum***

275 The experiment was conducted using divided Petri dishes, with a 1 cm diameter filter
276 paper was placed on one side and NB medium on the other. 3-methyl-1-butanol at
277 concentrations ranging from 100% purity to dilutions in dimethyl sulfoxide (DMSO)
278 were applied to the filter paper (20 μl per dish). 5 μl of *R. solanacearum* (OD_{600} = 0.5)
279 was inoculated onto the NB medium, and plates were incubated at 30°C for 48 h.
280 After incubation, 1 ml of sterile water was used to wash the bacterial colonies, and
281 then 50 μl of the bacterial suspension was diluted to 200 μl for OD_{600} measurements

282 using a SpectraMax M5 spectrophotometer (Molecular Devices, Sunnyvale, CA, USA).
283 DMSO was used as a blank control.

284 **RNA extraction and RNA-seq**

285 Total RNA was extracted from the bacterial cells using TRIzol® Reagent according the
286 manufacturer's instructions (Invitrogen, CA, USA). Then RNA quality was determined
287 using 2100 Bioanalyser (Agilent, CA, USA) and quantified using the ND-2000
288 (NanoDrop Technologies, DE, USA). RNA-seq strand-specific libraries were prepared
289 following TruSeq RNA sample preparation Kit from Illumina (San Diego, CA), using
290 5μg of total RNA. Shortly, rRNA removal by RiboZero rRNA removal kit (Epicenter,
291 Wisconsin, USA), fragmented using fragmentation buffer cDNA synthesis, end repair,
292 A-base addition and ligation of the Illumina-indexed adaptors were performed
293 according to Illumina's protocol. Libraries were then size selected for cDNA target
294 fragments of 200–300 bp on 2% Low Range Ultra Agarose followed by PCR amplified
295 using Phusion DNA polymerase (New England Biolabs, Massachusetts, USA) for 15
296 PCR cycles. After quantified by TBS380, paired-end libraries were sequenced by
297 Illumina NovaSeq 6000 sequencing (2 × 150bp, Shanghai BIOZERON Co., Ltd).
298 The raw paired end reads were trimmed and quality controlled by Trimmomatic with
299 parameters (SLIDINGWINDOW:4:15 MINLEN:75) (version 0.36
300 http://www.usadellab.org/cms/uploads/supplementary/Trimmomatic). Then clean
301 reads were separately aligned to reference genome with orientation mode using
302 Rockhopper (http://cs.wellesley.edu/~btjaden/Rockhopper/) software. Rockhopper
303 was a comprehensive and user-friendly system for computational analysis of
304 bacterial RNA-seq data. As input, Rockhopper takes RNA sequencing reads generated
305 by high-throughput sequencing technology. This software was used to calculate gene
306 expression levels with default parameters.

307 **Differential expression analysis and functional enrichment**

308 To identify differential expression genes (DEGs) between the two different samples,
309 the expression level for each transcript was calculated using the fragments per
310 kilobase of read per million mapped reads (RPKM) method. edgeR (52) was used for
311 differential expression analysis. The DEGs between two samples were selected using

312 the following criteria: the logarithmic of fold change was greater than 2 and the false
313 discovery rate (FDR) should be less than 0.05. To understand the functions of the
314 differential expressed genes, Gene Ontology (GO) functional enrichment and Kyoto
315 Encyclopedia and Genomes (KEGG) pathway analysis were carried out by Goatools
316 (53) and KOBAS (54) respectively. DEGs were significantly enriched in GO terms and
317 metabolic pathways when their Bonferroni-corrected P-value was less than 0.05.

318 **Data analysis and statistics**

319 All data analyses were performed using R version 4.3.1. Microbiome community
320 diversity was calculated as ASVs. Changes in community composition were assessed
321 with a principal component analysis (PCA) by using the R package "microceo" v1.9.0
322 (55), function adonis in R package "vegan" v2.6.4 (56) was conducted to evaluate the
323 significant difference in community structure across the different treatments. The
324 "ONE_Tukey_HSD2" function was uesd to compare the differences between different
325 treatments. The "LorMe" v1.1.0 package (57) in the laboratory was employed to
326 construct microbial co-occurrence networks. The "ComplexHeatmap" v1.10.2
327 package (58) was utilized to depict the heatmap of bacterial resource utilization
328 ability.

329 Results

330 **Inulin promotes the growth of HR92 and enhance its ability to control pathogens**

331 Screening experiments conducted in vitro indicated that none of the twelve
332 water-soluble sugar compounds tested promoted the growth of *R. solanacearum*
333 ($F_{13,28}$ = 8.483, p < 0.001, Fig. S1). Subsequently, the effects of these twelve sugars on
334 the growth and antimicrobial ability of HR92 were examined. It was found that inulin
335 had the most significant growth-promoting effect on HR92 ($F_{8,18}$ = 11.598, p < 0.001,
336 Fig. 1A), with an increase of up to 14.8%. Additionally, inulin significantly enhanced
337 HR92's inhibition of *R. solanacearum*, achieving the highest inhibition rate of 27.8%
338 ($F_{8,18}$ = 10.738, p < 0.001, Fig. 1B). Therefore, inulin was selected for subsequent pot
339 experiments to determine its impact on the disease suppression efficacy of HR92 at
340 different concentrations (Fig. S2).

341 Inoculation with HR92 resulted in a significant reduction in the disease index of
342 tomatoes, with the addition of inulin further decreasing the disease index. The
343 lowest disease index was observed in the treatment with 0.3% inulin, which achieved
344 a disease of 0.27, representing a 70% reduction compared to the control ($F_{3,12}$ =
345 45.34, $p < 0.05$, Fig. 1C). Similarly, the population of the *R. solanacearum* in the
346 rhizosphere exhibited a similar trend, with the lowest population detected following
347 the addition of 0.3% inulin, representing a two-order-of-magnitude reduction
348 compared to the pathogen-only treatment ($F_{3,12}$ = 46.95, $p < 0.05$, Fig. 1D). Notably,
349 HR92 alone did not efficiently colonize tomato roots ($F_{1,6}$ = 0.6, $p < 0.05$, Fig. 1E).
350 However, the addition of inulin significantly improved the colonization efficiency of
351 HR92 ($F_{3,12}$= 13.223, $p < 0.05$, Fig. 1E). While increasing the concentration of inulin
352 led to a slight increase in HR92 abundance in the rhizosphere, there was no
353 significant difference compared to the 0.1% inulin concentration ($F_{1,6}$ = 5.99, p =
354 0.068, Fig. 1E). Consistent with the in vitro findings, a 0.3% inulin concentration did
355 not further growth of HR92 compared to the 0.1% concentration ($F_{3,8}$ = 14.51, $p <$
356 0.05 , Fig. S3). The abundance of HR92 in the tomato rhizosphere was significantly
357 negatively correlated with both the disease severity index of tomatoes (R = -0.82 , $p <$
358 0.05) and the population of *R. solanacearum* (R = -0.9 , $p < 0.05$), indicating the
359 crucial role of HR92 in aiding tomato plants to resist pathogen invasion (Fig. S4).

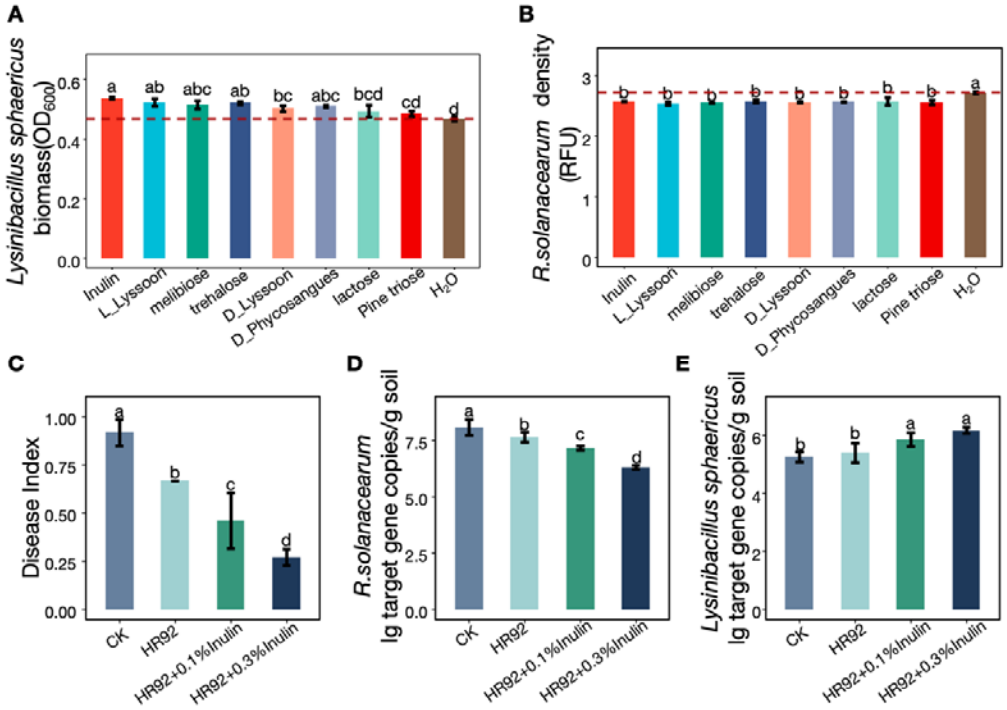

Fig. 1 Screening of sugar compounds and the effects of inulin and HR92 application on tomato bacterial wilt. (A) Growth response of HR92 to different water-soluble sugars, with the red dashed line representing the growth of HR92 in the absence of sugars (water control). (B) Inhibitory activity of HR92 against *R. solanacearum* in the presence of different water-soluble sugars, with the red dashed line representing HR92's baseline inhibitory capacity. (C) Tomato disease index under different treatments (N = 4). (D) Absolute abundance of *R. solanacearum* in the tomato rhizosphere under different treatments, quantified by qPCR using species-specific primers (one-way ANOVA with correction by Tukey's HSD test; N = 4). (E) Absolute abundance of HR92 in the tomato rhizosphere under different treatments, quantified by qPCR using species-specific primers (one-way ANOVA with correction by Tukey's HSD test; N = 4). Different letters in the bar graph indicate significant differences ($p < 0.05$).

HR92 and inulin alter the bacterial community of the tomato rhizosphere

16S rRNA gene amplicon sequencing was conducted to reveal the differences in the rhizosphere bacterial community among the four treatments. There were no significant differences in the Simpson and Shannon diversity indices between the control group and the HR92 or HR92+0.1% inulin treatment groups. However, the addition of 0.3% inulin with HR92 significantly decreased both the Simpson and Shannon indices of the tomato rhizosphere bacterial community (Shannon: $F_{3,12}$ = 9.26, p = 0.02, Fig 2A; Simpson $F_{3,12}$ = 3.36, p = 0.04, Fig 2B).

Principal coordinates analysis (PCoA) revealed significant differences in the bacterial community composition among the four treatments. Inoculating HR92 can alter the

tomato rhizosphere microbial community, and the addition of inulin can further modify the microbial community structure, with distinct differences observed between the 0.1% and 0.3% inulin treatments, being especially clear along the PCo1, which explained 29.1% of the total variation in bacterial community composition (PERMANOVA, R^2 = 0.460, p = 0.001, Fig. 2C).

Further analysis of the relative abundance of bacteria in different treatments revealed that bacteria amplicon sequence variants (ASVs) primarily belonged to 10 phyla, including *Proteobacteria*, *Acidobacteria*, *Bacteroidetes*, *Verrucomicrobia*, *Chloroflexi*, *Actinobacteria*, *Patescibacteria*, *Gemmatimonadetes*, *Myxococcota*, and *Firmicutes*. Although the composition of dominant bacterial phyla was similar across treatments, the relative abundance of certain dominant phyla differed significantly. Specifically, the phylum *Patescibacteria* was significantly enriched in the treatment with 0.3% inulin and HR92 (Fig. 2D).

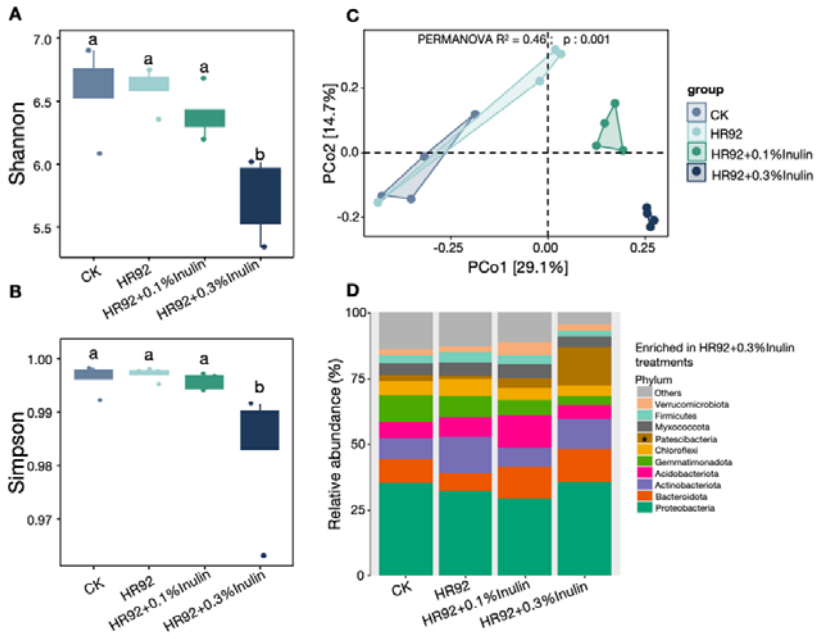

Fig. 2 Microbial community analysis under different treatments. (A) Alpha diversity analysis of the rhizosphere microbiome across treatments using the Shannon index. (B) Alpha diversity analysis using the Simpson index. (C) PCoA of the rhizosphere soil microbiota under each treatment. (D) Relative abundance of the top 10 most abundant phyla in the rhizosphere soil across treatments. The asterisk indicates phyla enriched specifically in the HR92+0.3% inulin treatment compared to the other treatments. Different letters above the boxes of each compartment indicate a significant difference at $p < 0.05$ (one-way ANOVA with correction by Tukey's HSD test).

Inulin stimulates native soil resident microbes to assist HR92 in resisting *R.*

404 ***solanacearum* invasion**

405 Following the application of 0.3% inulin in combination with HR92, the colonization
406 of HR92 in the rhizosphere did not significantly increase (Fig. 1E). However, the
407 disease index of tomatoes and the population of rhizosphere *R. solanacearum*
408 further decreased (Fig. 1C, D). We hypothesize that, beyond its direct effect on HR92,
409 the 0.3% inulin may enrich certain native soil resident microbes that contribute to
410 pathogen suppression. Subsequently, 21 genera significantly enriched in the
411 treatment with 0.3% inulin were identified, defining them as potential key taxa (Table
412 S1, $p < 0.05$).

413 Further analysis of co-occurrence networks and distribution patterns of dominant
414 genera across the four treatments identified key taxa. Notably, among the top ten
415 nodes in the co-occurrence network based on betweenness centrality, two ASVs,
416 ASV2 (*Pseudarthrobacter*) and ASV201(*Agromyces*), were recognized as potential
417 keystone bacteria (Fig. 3A). The relative abundance of ASV2 was significantly
418 correlated with inulin concentration, with its abundance further increasing under the
419 0.3% inulin treatment, whereas ASV201 was enriched exclusively in the 0.3% inulin
420 treatment (ASV2: $F_{3,12} = 13.16$, $p < 0.001$; ASV201: $F_{3,12} = 19.18$, $p < 0.001$, Fig. 3B).
421 Both ASV2 (R = -0.82, $p < 0.05$) and ASV201 (R = -0.81, $p < 0.05$) exhibited significant
422 negative correlations with the abundance of *R. solanacearum*, and
423 *Pseudarthrobacter* ($R = -0.77$, $p < 0.05$) and *Agromyces* ($R = -0.75$, $p < 0.05$) also
424 demonstrated significant negative correlations with the abundance of *R.*
425 *solanacearum* (Fig. S5A, B). Thus, *Pseudarthrobacter* and *Agromyces* are considered
426 potential key taxa that interact synergistically with HR92 to confer disease resistance.

427 Additionally, microorganisms enriched under the 0.3% inulin treatment were
428 predominantly concentrated within modules 2 and 3 of the co-occurrence network,
429 both of which were significantly negatively correlated with pathogen abundance
430 (module 2: $R = -0.69$, $p < 0.05$; module 3: $R = -0.82$, $p < 0.05$; Fig. S5C, D), suggesting
431 their crucial roles in disease suppression.

432 Tax4Fun functional prediction indicated that *Pseudarthrobacter* is primarily
433 associated with secondary metabolite synthesis, basic metabolism, and isoflavonoid

biosynthesis, suggesting that *Pseudarthrobacter* may mediate disease resistance via these pathways (Fig. S6). Given its significant association with disease suppression and its tenfold higher abundance compared to *Agromyces* in the tomato rhizosphere, *Pseudarthrobacter* likely plays a more prominent role in mediating rhizosphere interactions. Therefore, subsequent validation experiments focused on *Pseudarthrobacter*.

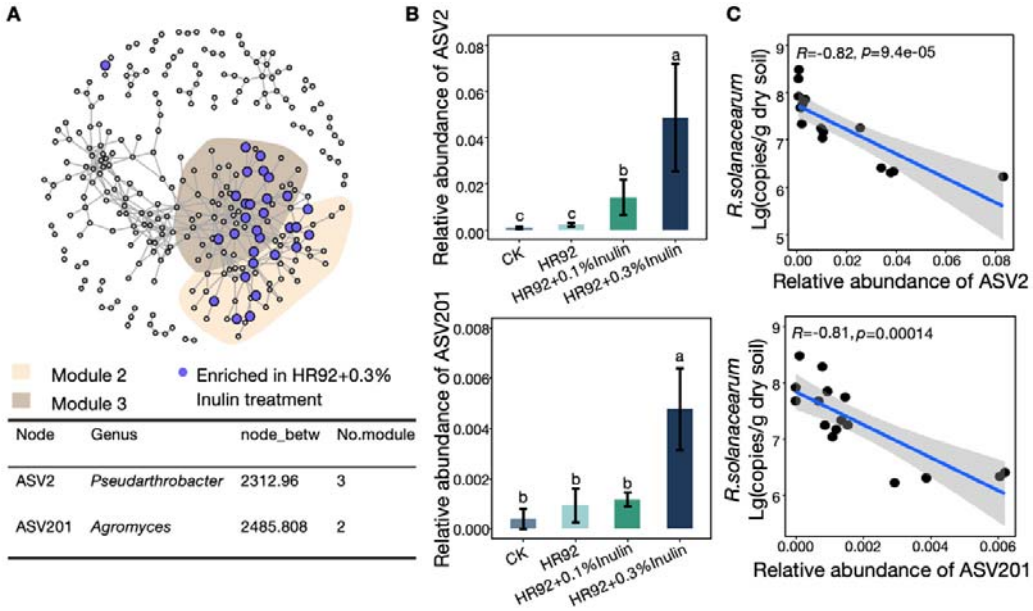

Fig. 3 Co-occurrence network analysis. (A) The co-occurrence network at the ASV level, where the purple nodes represent ASVs enriched under high-concentration inulin treatment. Key nodes and their properties are detailed below the network graph. (B) Relative abundance of ASV2 and ASV201 in the rhizosphere microbial communities across four treatments (N = 4; one-way ANOVA with correction by Tukey's HSD test). (C) Linear regression between the relative abundance of ASV2 and ASV201 and the population of *R.solanacearum* in the tomato rhizosphere ($p < 0.05$). Different letters in the graph indicate significant differences ($p < 0.05$).

Pseudarthrobacter strains in cooperative interaction with HR92 to suppress _R. solanacearum_ invasion

We isolated eight representative strains of *Pseudarthrobacter* spp. from soil treated with 0.3% inulin for subsequent in vitro validation. Two strains with significant results, *Pseudarthrobacter siccitolerans* P265 and *Pseudarthrobacter oxydans* P397, were selected for further characterization (Fig. S7). Inulin significantly promoted the growth of strain P265 and P397 (strain P265: t-test: $t_{6.32}$ = -2.82, p = 0.029; strain P397: t-test: $t_{8.67}$ = -6.42, $p < 0.001$; Fig. 4A), indicating that these bacteria effectively utilized inulin as a resource. We subsequently assessed the potential of strain P265

457 and P397 to inhibit pathogenic activity. In vitro assays demonstrated that the
458 supernatants from P265 and P397 did not directly inhibit *R. solanacearum* (strain
459 P265: $F_{2,11}$ = 0.69, p = 0.5; strain P397: $F_{2,11}$ = 1.15, p = 0.5, Fig. S8). However, under
460 co-culture conditions, both P265 and P397 inhibited the growth of *R. solanacearum*,
461 the inhibition rate of P265 was 41%, and that of P397 was 41.4%, with the addition
462 of inulin showing no significant influence on this inhibitory effect (strain P265: $F_{2,9}$ =
463 130.13, p < 0.001; strain P397: $F_{2,9}$ = 56.58, p < 0.001; Fig. 4B). These observations
464 suggest that the inhibitory mechanism may involve nutrient competition between
465 these strains and *R. solanacearum*.
466 To explore nutrient competition we examined the utilization of 74 different
467 rhizosphere carbon sources by P265, P397, and *R. solanacearum*. The results
468 indicated that P265 and P397 utilized a broader range of resources compared to *R.*
469 *solanacearum* (Fig. S9、Table 2, p < 0.05). The overlap in resource utilization between
470 P265 and *R. solanacearum* was 0.94, and between P397 and *R. solanacearum* was
471 0.91 (Fig. 4C), indicating potential competition for carbon resources between
472 *Pseudarthrobacter* strains and *R. solanacearum*.
473 Additionally, the supernatant from the co-culture of strain HR92 with P265 or P397
474 showed an enhanced inhibitory effect against *R. solanacearum* (strain P265: $F_{3,12}$ =
475 19.18, p < 0.001; strain P397: $F_{3,12}$ = 22.35, p < 0.001; Fig. 4D). We hypothesized that
476 either strain HR92 induced antibacterial activity in strains P265 and P397 or that
477 these strains augmented strain HR92's antibacterial function. To test this hypothesis,
478 first, we fed the supernatant of strain HR92 to P265 and P397. Subsequently, we fed
479 the supernatants of P265 and P397 to *R. solanacearum* and found that the growth of
480 *R. solanacearum* was not affected (strain P265: $F_{2,18}$ = 1.834, p = 0.18; strain P397:
481 $F_{2,18}$ = 1.55, p = 0.24, Fig. S10). This indicates that strain HR92 was unable to confer
482 the ability to antagonize *R. solanacearum* to P265 or P397. Conversely, we fed the
483 supernatant of strain P265 or P397 to strain HR92 and found that the supernatant of
484 strain HR92 had a stronger ability to inhibit *R. solanacearum*, with enhancements of
485 12% and 6.6%, respectively (strain P265: $F_{2,9}$ = 46.23, p < 0.001; strain P397: $F_{2,9}$ =

33.306, $p < 0.001$; Fig. 4E). In pot experiments, consistent with the in vitro findings, strains P265 and P397 enhanced the ability of strain HR92 to mitigate tomato bacterial wilt. Notably, the combined treatment of strain HR92, *Pseudarthrobacter* strains, and inulin provided the best protection against tomato bacterial wilt, with a disease index of 0.3375 (P265) and 0.35 (P397), achieving control efficiencies of 61.9% (P265) and 60.5% (P397) ($F_{6,21} = 87.21$, $p < 0.001$, Fig. 4F).

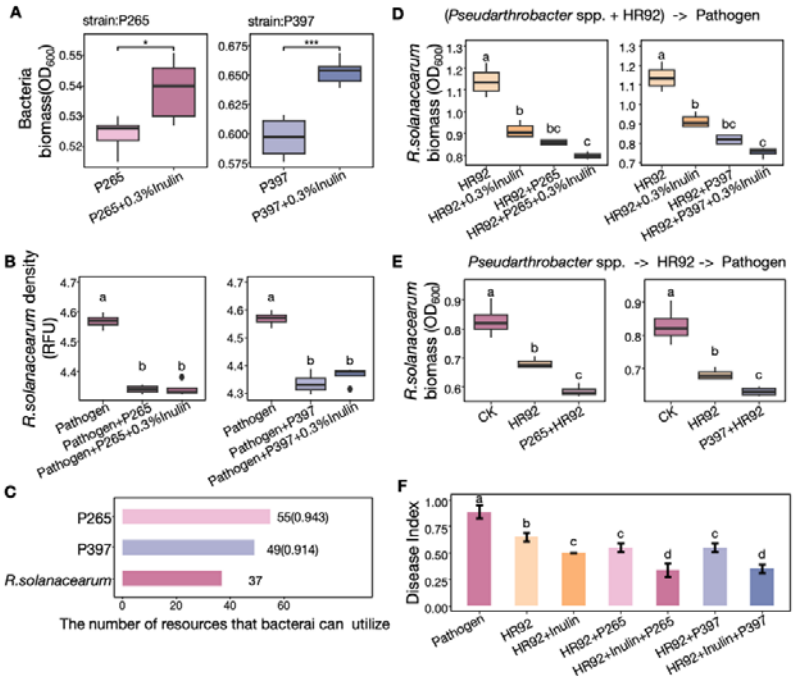

Fig. 4 Investigation of the antibacterial effects of *Pseudarthrobacter* spp. and its influence on the antibacterial activity of HR92. (A) Effect of inulin on the growth of *Pseudarthrobacter siccitolerans* (P265) and *Pseudarthrobacter oxydans* (P397). Asterisk means $p < 0.05$ and three asterisks means $p < 0.001$ under student's t test ($N = 4$). (B) Inhibition of *R. solanacearum* by strains P265 and P397 under co-culture conditions with and without the addition of inulin. (C) Resource utilization overlap between strain P265/P397 and *R. solanacearum*, indicating the potential nutritional competition. (D) Enhanced antibacterial activity of the supernatant after co-culture of strain HR92 with strains P265 and P397. The arrows at the top of the box plot represent the feeding procedure. Specifically, they indicate feeding the pathogen with the supernatant from co-cultures of strain P267 or P397 and strain HR92. (E) Increased antibacterial activity of HR92 after being cultured with the supernatants from strains P265/P397. The arrows at the top of the box plot represent the feeding procedure. Specifically, they indicate feeding strain HR92 with the supernatant from strain P267 or P397, followed by feeding the pathogen with the supernatant from strain HR92. (F) Pot experiments showing enhanced tomato disease resistance when HR92, *Pseudarthrobacter* strains, and inulin were applied together. Different letters in the graph indicate significant differences ($p < 0.05$).

***Pseudarthrobacter* strains and inulin enhance HR92's synthesis of cyclic lipopeptide**

510 **surfactin and 3-methyl-1-butanol**

511 Transcriptomic analysis was conducted to elucidate the individual and combined
512 effects of inulin and *Pseudarthrobacter* strains on strain HR92. Inulin upregulated
513 genes involved in flagellar assembly, bacterial chemotaxis, fatty acid biosynthesis,
514 and siderophore biosynthesis in strain HR92, indicating that inulin enhances the
515 motility of HR92 in the rhizosphere, thereby increasing its colonization quantity(Fig.
516 S11). Strains P265 and P397 collectively influenced genes expression in strain HR92,
517 with significant differential expression observed in genes related to the synthesis of
518 4-aminobutyrate, methyl-accepting, butanediol and bacitracin, all of which are
519 associated with strain HR92's antimicrobial activity (Fig. S12). Bacitracin is a
520 broad-spectrum antibiotic known for its antimicrobial properties. Furthermore, the
521 combined action of *Pseudarthrobacter* strains and inulin enhanced the synthesis of
522 amino acids such as valine and leucine in HR92 (Fig. S13, Fig. S14). Subsequent
523 Weighted Gene Co-expression Network Analysis (WGCNA) identified three gene
524 modules in strain HR92 that were linked to its antimicrobial activity (Fig. S15). Within
525 the black and pink modules, two genes highly correlated with the modules and
526 exhibiting the highest correlation with strain HR92's antimicrobial effect were
527 identified: LYS2002816 and LYS2001501. These genes were associated with
528 butanediol and NAD(P)H, both of which exhibited a significant positive correlation
529 with strain HR92's antimicrobial capability (LYS2002816: R = 0.79, p <0.05,
530 LYS2001501: R = 0.73, p <0.05, Fig. S16). The abundance of these genes was highest
531 in strain P265 or P397, HR92, and inulin treatment (LYS2002816: $F_{5,12}$ = 2.9, p < 0.05,
532 Figure 5A; LYS2001501: $F_{5,12}$ = 5.8, p < 0.05, Figure 5B). Literature review indicated
533 that butanediol contributes to the synthesis of the volatile antimicrobial compound
534 3-methyl-1-butanol in strain HR92, whereas fatty acids, NAD(P)H, valine, and leucine
535 are involved in the synthesis of the cyclic lipopeptide surfactin (Fig. 5C, D), ultimately
536 enhancing strain HR92's ability to inhibit *R. solanacearum*.

537 To further elucidate the role of 3-methyl-1-butanol, we tested its effect on *R.*
538 *solanacearum* growth. Our results showed that 50% and 100% concentrations of
539 3-methyl-1-butanol could inhibit the growth of *R. solanacearum*, with 50%

540 concentration resulting in a 16.4% inhibition rate and 100% concentration achieving
541 a 40% inhibition rate ($F_{4,10}$ = 6.839, $p < 0.05$, Fig. S17).

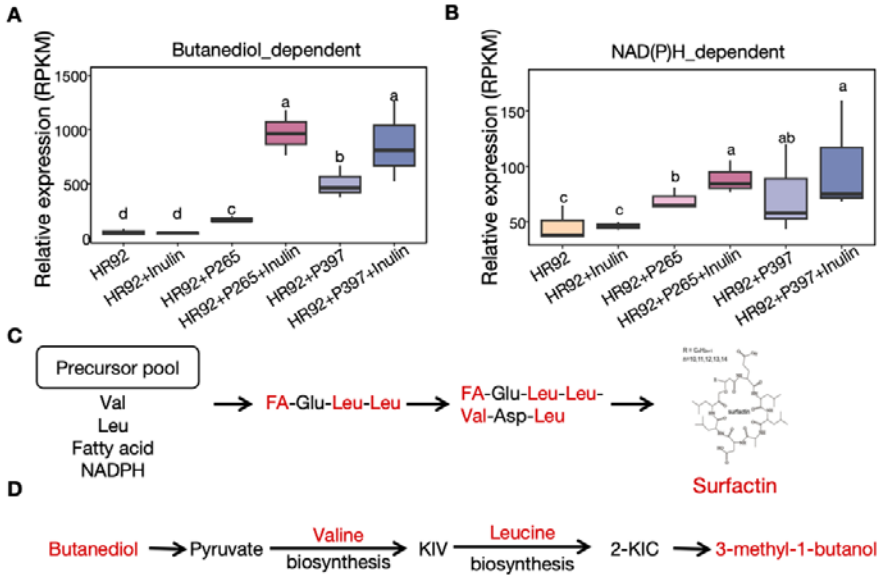

542

543 Fig. 5 Synergistic enhancement of HR92 antibacterial capability by *Pseudarthrobacter* spp. and
544 inulin. (A) Expression levels of HR92 genes associated with butanediol synthesis across six
545 treatments, quantified by RPKM tables. (B) Expression levels of HR92 genes involved in NAD(P)H
546 synthesis across six treatments, quantified by RPKM tables. Different letters in the graph indicate
547 significant differences (Duncan's multiple range test). (C) Schematic diagram illustrating the
548 involvement of fatty acids, NAD(P)H, valine, and leucine in the biosynthesis of the cyclic
549 lipopeptide surfactin. (D) Schematic diagram showing the pathway through which butanediol is
550 converted to 3-methyl-1-butanol via pyruvate, valine biosynthesis, and leucine biosynthesis
551 pathways. Red font highlights the pathways or genes influenced by the synergistic action of
552 *Pseudarthrobacter* spp. and inulin.

553 **Discussion**

554 There is growing interest in harnessing beneficial bacteria for plant disease
555 biocontrol, yet strategies to maxmize their effectiveness remain insufficiently
556 explored. Here, our study emphasizes the important role of inulin in promoting the
557 growth and pathogen-suppressing capabilities of the beneficial strain HR92, along
558 with its synergistic interactions with native soil microbes to manage *R. solanacearum*
559 infections in tomatoes. We also investigated whether increased inulin
560 concentrations could further improve the biocontrol efficacy of strain HR92. Both *in*
561 *vitro* and *in vivo* experiments demonstrated that inulin positively influenced bacterial
562 colonization and biocontrol efficiency. In general, higher inulin concentrations

563 selectively enriched *Pseudarthrobacter* species in the soil, which acted synergistically
564 with strain HR92 to enhance biocontrol outcomes.
565 Inulin promoted strain HR92 growth and augmented its pathogen-suppressing ability.
566 Initially, we observed a threefold increase in strain HR92 population in the tomato
567 rhizosphere upon inulin treatment. This finding is consistent with previous studies
568 showing that inulin selectively stimulates the growth of beneficial bacteria, such as
569 *Bifidobacterium*, *Lactobacillus*, and *Bacteroides,* while inhibiting potential pathogens
570 (59). Additionally, inulin has been shown to increase the production of lactic acid,
571 acetic acid, and other volatile compounds by probiotic strains, indicating a positive
572 synergistic interaction between inulin and beneficial microbes (60). These findings
573 support our results that inulin, as a prebiotic, promotes the growth of beneficial
574 bacteria. We further discovered that the disease severity index for tomatoes treated
575 with both inulin and strain HR92 decreased by 31.2% compared to those treated with
576 strain HR92 alone. Previous research has demonstrated that strain HR92 could
577 effectively control *R. solanacearum* (19), suggesting a direct impact of strain HR92 on
578 the *R. solanacearum*. This can be interpreted as the biocontrol efficacy of beneficial
579 bacteria being closely related to their abundance in the rhizosphere (61), and that
580 plant-derived carbon sources could enhance the metabolic activity of specific
581 beneficial bacteria, thereby improving their disease resistance (62, 63). Furthermore,
582 we observed that increasing the inulin concentration from 0.1% to 0.3% did not
583 further promote the growth of strain HR92, which may be due to strain HR92 already
584 obtaining sufficient nutrients at the 0.1% concentration. The optimal inulin
585 concentration for promoting strain HR92 growth under complex environmental
586 conditions remains to be further investigated.
587 Inulin and its varying concentrations significantly influenced rhizosphere microbial
588 diversity and community structure. While a low inulin concentration (0.1%) had no
589 significant effect on the Simpson and Shannon diversity indices, a higher
590 concentration (0.3%) reduced these indices. This can be explained by higher
591 concentrations of inulin potentially altering community structure by selectively
592 enriching certain functional bacteria, thereby reducing the relative abundance of

593 other bacterial groups. Our findings revealed distinct differences in bacterial
594 community composition between the two inulin concentrations treatments. Previous
595 studies have indicated that the concentration of exogenous carbon sources in soil has
596 a significant selective effect on native microbial communities (40, 64). Taken together,
597 different concentrations of inulin can regulate the interactions and structure of
598 native microbial communities, maintaining higher diversity at lower concentrations
599 while promoting the enrichment of specific functional bacteria at higher
600 concentrations. Since a higher concentration of inulin further reduced disease
601 severity and the abundance of *R. solanacearum* in the rhizosphere, without altering
602 the abundance of strain HR92 in the rhizosphere. Therefore, we hypothesize that,
603 beyond directly benefiting strain HR92, a 0.3% inulin concentration may also enrich
604 certain native soil microbes that aid in suppressing pathogens. In fact, in the
605 co-occurrence network analysis, *Pseudoarthrobacter* and *Agromyces* were
606 significantly enriched under high inulin concentration treatment and identified as key
607 network hubs, rowten showing a significant negative correlation with the pathogen.
608 This suggests that they may support strain HR92's pathogen suppression function
609 through competition or antagonistic interactions. Interestingly, previous studies have
610 indicated that *Pseudoarthrobacter* is adept at collaborating with other beneficial
611 bacteria to perform better ecological functions (65). On the other hand, strains
612 belonging to the genus *Pseudoarthrobacter* are known as copiotrophic root
613 colonizers (66, 67) and have been proposed as a key members of the root
614 microbiome (68). In summary, the present study highlights the importance of the
615 synergistic interaction between inulin, *Pseudoarthrobacter* and HR92 in managing
616 *Ralstonia solanacearum*.
617 Our study also demonstrates that the combined effects of inulin and
618 *Pseudoarthrobacter* strains significantly enhance the antibacterial activity of HR92
619 against *R. solanacearum*, primarily through the upregulation of genes related to the
620 synthesis of key metabolites, such as surfactin and 3-methyl-1-butanol. The
621 inhibitory effects of these metabolites on pathogens have been well-documented.
622 The cyclic lipopeptide surfactin, a polypeptide compound composed of fatty acids

623 and amino acids, exhibits notable antimicrobial, antiviral, and plant
624 stress-resistance-promoting activities, playing a particularly prominent role in disease
625 defense (69). Transcriptomic analysis in this study revealed that inulin and
626 *Pseudoarthrobacter* strains promoted the synthesis of surfactin by upregulating
627 metabolic pathways related to fatty acids and amino acids, such as valine and leucine.
628 Furthermore, 3-methyl-1-butanol, as a volatile antimicrobial compound, has shown
629 high efficacy in inhibiting various pathogens. Its mode of action involves binding to
630 microbial cell membranes, inserting into the bilayer structure, and altering
631 membrane permeability, which destabilizes the membrane, causes leakage of cellular
632 contents such as ions and ATP, and ultimately leads to cell death, effectively inhibiting
633 pathogen growth (70, 71). Our co-expression network analysis of HR92 genes
634 indicated that the butanediol and NADPH metabolic pathways are closely associated
635 with the antibacterial potential of HR92, possibly by promoting the synthesis of
636 3-methyl-1-butanol. Further experimental validation confirmed that high
637 concentrations of 3-methyl-1-butanol exhibit strong inhibitory effects on *R.*
638 *solanacearum*, which is consistent with other studies on volatile organic compounds
639 (VOCs) as disease suppressants (72). In summary, these results suggest that the
640 synergistic effects of inulin and *Pseudoarthrobacter* can significantly enhance HR92's
641 ability to suppress *R. solanacearum* by promoting the synthesis of key antibacterial
642 metabolites.
643 In conclusion, our study demonstrates that the inulin significantly enhances strain
644 HR92 colonization, chemotaxis, fatty acid metabolism, and siderophore production in
645 tomato roots. The addition of 0.3% inulin had a greater impact than 0.1%, notably
646 enriching *Pseudoarthrobacter* species within the rhizosphere. These species
647 promoted the synthesis of butanediol and bacitracin in strain HR92, thereby
648 enhancing its antimicrobial capabilities. Furthermore, *Pseudoarthrobacter* spp.
649 competed with *R. solanacearum* for root-associated resources, reducing the
650 abundance of pathogenic bacteria via nutrient competition. The combined effects of
651 *Pseudarthrobacter* spp. and inulin further upregulated strain HR92's valine and
652 leucine metabolic pathways. Valine, leucine, fatty acids, and NAD(P)H are essential

precursors for *L. sphaericus* to synthesize the antimicrobial cyclic lipopeptide surfactin. Additionally, butanediol is converted into the antimicrobial VOC 3-methyl-1-butanol through valine and leucine metabolic pathways. Thus, the cooperative interaction between *Pseudoarthrobacter* spp. and inulin enhanced strain HR92's ability to inhibit *R. solanacearum*, ultimately reducing the incidence of tomato disease. This research provides valuable insights into the synergistic interactions between exogenous additives and beneficial microbes, offering a foundation for developing advanced, targeted formulations for sustainable and effective disease management (Fig 6).

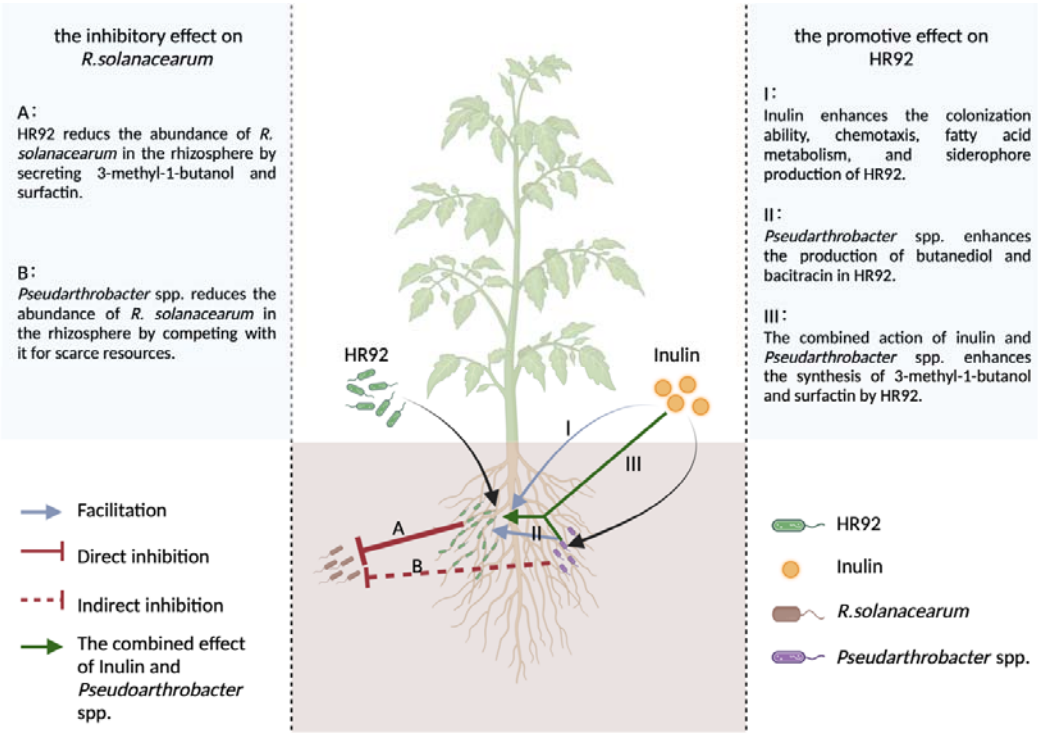

Fig. 6 Pathways by which inulin enhances HR92's disease-resistance mechanisms. Blue arrows indicate promotion effects, red solid lines indicate direct inhibition effects, red dashed lines indicate inhibition of pathogen growth through nutrient competition.

Data availability

All metagenomics reads are publicly available in the SRA database under the accession number PRJNA1198698.

Acknowledgments

This study was funded by the National Natural Science Foundation of China

(42477125, 42325704, and 42090060), the Fundamental Research Funds for the Central Universities (KYT2024001), the Natural Science Foundation of Jiangsu Province (BK20230988), the Jiangsu Carbon Peak & Carbon Neutrality Science and Technology Innovation Special Fund (BE2022423), and the National Key Research and Development Program of China (2024YFC3406000).

Conflict of Interest

The authors declare no competing interests.

680 ## References

681 1. Liu J, Yao Q, Li Y, Zhang W, Mi G, Chen X, Yu Z, Wang G. 2019. Continuous cropping of
682 soybean alters the bulk and rhizospheric soil fungal communities in a Mollisol of Northeast
683 PR China. Land Degrad Dev 30:1725–1738.

684 2. Zheng GD, Shi LB, Wu HY, Peng DL. 2012. Nematode communities in continuous
685 tomato-cropping field soil infested by root-knot nematodes. Acta Agriculturae Scandinavica,
686 Section B - Soil & Plant Science 62:216–223.

687 3. Tsiafouli MA, Thébault E, Sgardelis SP, De Ruiter PC, Van Der Putten WH, Birkhofer K,
688 Hemerik L, De Vries FT, Bardgett RD, Brady MV, Bjornlund L, Jørgensen HB, Christensen S,
689 Hertefeldt TD, Hotes S, Gera Hol WH, Frouz J, Liiri M, Mortimer SR, Setälä H, Tzanopoulos J,
690 Uteseny K, Pižl V, Stary J, Wolters V, Hedlund K. 2015. Intensive agriculture reduces soil
691 biodiversity across Europe. Global Change Biology 21:973–985.

692 4. Raaijmakers JM, Mazzola M. 2016. Soil immune responses. Science 352:1392–1393.

693 5. Delgado-Baquerizo M, Guerra CA, Cano-Díaz C, Egidi E, Wang J-T, Eisenhauer N, Singh BK,
694 Maestre FT. 2020. The proportion of soil-borne pathogens increases with warming at the
695 global scale. Nat Clim Chang 10:550–554.

696 6. Andreote FD, Pereira E Silva MDC. 2017. Microbial communities associated with plants:
697 learning from nature to apply it in agriculture. Current Opinion in Microbiology 37:29–34.

698 7. Yuan W, Ruan S, Qi G, Wang R, Zhao X. 2022. Plant growth-promoting and antibacterial
699 activities of cultivable bacteria alive in tobacco field against *Ralstonia solanacearum*.

700 Environmental Microbiology 24:1411–1429.

701 8. Sanguin H, Sarniguet A, Gazengel K, Moënne-Loccoz Y, Grundmann GL. 2009. Rhizosphere
702 bacterial communities associated with disease suppressiveness stages of take-all decline in
703 wheat monoculture. New Phytologist 184:694–707.

704 9. Zhou X, Wang J, Liu F, Liang J, Zhao P, Tsui CKM, Cai L. 2023. Author Correction:
705 Cross-kingdom synthetic microbiota supports tomato suppression of *Fusarium* wilt disease.
706 Nat Commun 14:6755.

707 10. Li M, Pommier T, Yin Y, Wang J, Gu S, Jousset A, Keuskamp J, Wang H, Wei Z, Xu Y, Shen Q,
708 Kowalchuk GA. 2022. Indirect reduction of *Ralstonia solanacearum* via pathogen helper
709 inhibition. ISME J 16:868–875.

710 11. Wu B, Wang X, Yang L, Yang H, Zeng H, Qiu Y, Wang C, Yu J, Li J, Xu D, He Z, Chen S. 2016.
711 Effects of Bacillus amyloliquefaciens ZM9 on bacterial wilt and rhizosphere microbial
712 communities of tobacco. Applied Soil Ecology 103:1–12.

713 12. Wang N, Ding J, Chen Y, Zhu Y, Zhang L, Wei Y, Li J, Xu T, Ding G. 2023. *Bacillus velezensis*
714 BER1 enriched *Flavobacterium daejeonense* -like bacterium in the rhizosphere of tomato
715 against bacterial wilt. FEMS Microbiology Ecology 99:fiad054.

716 13. Wang X, Li G-H, Zou C-G, Ji X-L, Liu T, Zhao P-J, Liang L-M, Xu J-P, An Z-Q, Zheng X, Qin Y-K,
717 Tian M-Q, Xu Y-Y, Ma Y-C, Yu Z-F, Huang X-W, Liu S-Q, Niu X-M, Yang J-K, Huang Y, Zhang K-Q.
718 2014. Bacteria can mobilize nematode-trapping fungi to kill nematodes. Nat Commun
719 5:5776.

720 14. Wei Z, Yang T, Friman V-P, Xu Y, Shen Q, Jousset A. 2015. Trophic network architecture of
721 root-associated bacterial communities determines pathogen invasion and plant health. Nat
722 Commun 6:8413.

723 15. Hase S, Shimizu A, Nakaho K, Takenaka S, Takahashi H. 2006. Induction of transient ethylene
724 and reduction in severity of tomato bacterial wilt by *Pythium oligandrum*. Plant Pathology
725 55:537–543.

726 16. Sakthivel K, Manigundan K, Gautam RK, Singh PK, Balamurugan A, Kumar A, Sharma SK.
727 2023. Microbe-enriched farm yard manure (MFYM) approach for the suppression of
728 Ralstonia solanacearum Yabuuchi (Smith) inciting bacterial wilt disease in eggplant
729 (*Solanum melongena L.*). Plant Soil 491:303–315.

730 17. Jamal QMS, Ahmad V. 2022. Lysinibacilli: A Biological Factories Intended for Bio-Insecticidal,
731 Bio-Control, and Bioremediation Activities. JoF 8:1288.

732 18. Shabanamol S, Thampi M, Sajana P, Varghese S, Karthika S, George TK, Jisha MS. 2021.
733 Characterization of the major antifungal extrolite from rice endophyte *Lysinibacillus*
734 *sphaericus* against Rhizoctonia solani. Arch Microbiol 203:2605–2613.

735 19. Huang J, Wei Z, Tan S, Mei X, Yin S, Shen Q, Xu Y. 2013. The rhizosphere soil of diseased
736 tomato plants as a source for novel microorganisms to control bacterial wilt. Applied Soil
737 Ecology 72:79–84.

738 20. Yoon, M.Y. Lysinibacillus sphaericus TC1 Strain and Method for Controlling Plant Diseases
739 Using the Same. Patent Application No. KR20140051676A, 2 May 2014.

740 21. Akintayo SO, Treinen C, Vahidinasab M, Pfannstiel J, Bertsche U, Fadahunsi I, Oellig C,
741 Granvogl M, Henkel M, Lilge L, Hausmann R. 2022. Exploration of surfactin production by
742 newly isolated *Bacillus* and *Lysinibacillus* strains from food-related sources. Letters in
743 Applied Microbiology 75:378–387.

744 22. Zhi Y, Wu Q, Xu Y. 2017. Genome and transcriptome analysis of surfactin biosynthesis in
745 *Bacillus amyloliquefaciens* MT45. Sci Rep 7:40976.

746 23. Sakthivel K, Manigundan K, Gautam RK, Singh PK, Yogeshwari, Subramani T, Sharma SK,
747 Khande R. 2018. Bioefficacy of antimicrobial peptide biosynthesis-gene-linked antagonistic
748 *Lysinibacillus sphaericus* strains for management of bacterial plant diseases in Andaman
749 and Nicobar Islands, India. JEB 39:517–521.

750 24. Wei Z, Huang J, Yang T, Jousset A, Xu Y, Shen Q, Friman V-P. 2017. Seasonal variation in the
751 biocontrol efficiency of bacterial wilt is driven by temperature-mediated changes in
752 bacterial competitive interactions. J Appl Ecol 54:1440–1448.

753 25. El-Hassan SA, Gowen SR. 2006. Formulation and Delivery of the Bacterial Antagonist
754 *Bacillus subtilis* for Management of Lentil Vascular Wilt Caused by *Fusarium oxysporum* f. sp.
755 *lentis*. Journal of Phytopathology 154:148–155.

756 26. Albright MBN, Louca S, Winkler DE, Feeser KL, Haig S-J, Whiteson KL, Emerson JB, Dunbar J.
757 2022. Solutions in microbiome engineering: prioritizing barriers to organism establishment.
758 The ISME Journal 16:331–338.

759 27. Kaminsky LM, Trexler RV, Malik RJ, Hockett KL, Bell TH. 2019. The Inherent Conflicts in

760 Developing Soil Microbial Inoculants. Trends in Biotechnology 37:140–151.

761 28. El Fantroussi S, Agathos SN. 2005. Is bioaugmentation a feasible strategy for pollutant
762 removal and site remediation? Current Opinion in Microbiology 8:268–275.

763 29. Tao C, Li R, Xiong W, Shen Z, Liu S, Wang B, Ruan Y, Geisen S, Shen Q, Kowalchuk GA. 2020.
764 Bio-organic fertilizers stimulate indigenous soil Pseudomonas populations to enhance plant
765 disease suppression. Microbiome 8:137.

766 30. Gu Y, Hou Y, Huang D, Hao Z, Wang X, Wei Z, Jousset A, Tan S, Xu D, Shen Q, Xu Y, Friman V-P.
767 2017. Application of biochar reduces *Ralstonia solanacearum* infection via effects on
768 pathogen chemotaxis, swarming motility, and root exudate adsorption. Plant Soil
769 415:269–281.

770 31. Jin X, Rahman MKU, Ma C, Zheng X, Wu F, Zhou X. 2023. Silicon modification improves
771 biochar's ability to mitigate cadmium toxicity in tomato by enhancing root colonization of
772 plant-beneficial bacteria. Ecotoxicology and Environmental Safety 249:114407.

773 32. Wang X, Zhang Y, Xu W, Cheng J, Liu J, Pei W, Wang J, Chuang S. 2023. Amino acid fertilizer
774 strengthens its effect on crop yield and quality by recruiting beneficial rhizosphere
775 microbes. J Sci Food Agric 103:5970–5980.

776 33. Hu Y, Li Y, Yang X, Li C, Wang L, Feng J, Chen S, Li X, Yang Y. 2021. Effects of integrated
777 biocontrol on bacterial wilt and rhizosphere bacterial community of tobacco. Sci Rep
778 11:2653.

779 34. Yuan S, Wang L, Wu K, Shi J, Wang M, Yang X, Shen Q, Shen B. 2014. Evaluation of
780 Bacillus-fortified organic fertilizer for controlling tobacco bacterial wilt in greenhouse and
781 field experiments. Applied Soil Ecology 75:86–94.

782 35. Matsuzaki C, Takagi H, Saiga S, Kinoshita Y, Yamaguchi M, Higashimura Y, Yamamoto K,
783 Yamaguchi M. 2024. Prebiotic effect of galacto- *N* -biose on the intestinal lactic acid
784 bacteria as enhancer of acetate production and hypothetical colonization. Appl Environ
785 Microbiol e01445-23.

786 36. Bertelsen RJ, Jensen ET, Ringel-Kulka T. 2016. Use of probiotics and prebiotics in infant
787 feeding. Best Practice & Research Clinical Gastroenterology 30:39–48.

788 37. Sánchez ÓJ, Ospina DA, Montoya S. 2017. Compost supplementation with nutrients and
789 microorganisms in composting process. Waste Management 69:136–153.

790 38. Xiong Q, Liu D, Zhang H, Dong X, Zhang G, Liu Y, Zhang R. 2020. Quorum sensing signal
791 autoinducer-2 promotes root colonization of *Bacillus velezensis* SQR9 by affecting biofilm
792 formation and motility. Appl Microbiol Biotechnol 104:7177–7185.

793 39. Xu Z, Zhang H, Sun X, Liu Y, Yan W, Xun W, Shen Q, Zhang R. 2019. *Bacillus velezensis* Wall
794 Teichoic Acids Are Required for Biofilm Formation and Root Colonization. Appl Environ
795 Microbiol 85:e02116-18.

796 40. Wen T, Xie P, Liu H, Liu T, Zhao M, Yang S, Niu G, Hale L, Singh BK, Kowalchuk GA, Shen Q,
797 Yuan J. 2023. Tapping the rhizosphere metabolites for the prebiotic control of soil-borne
798 bacterial wilt disease. Nat Commun 14:4497.

799 41. Xu Z, Xie J, Zhang H, Wang D, Shen Q, Zhang R. 2019. Enhanced Control of Plant Wilt
800 Disease by a Xylose-Inducible *degQ* Gene Engineered into *Bacillus velezensis* Strain
801 SQR9XYQ. Phytopathology® 109:36–43.

802 42. Kim L, Mogk A, Schumann W. 1996. A xylose-inducible *Bacillus subtilis* integration vector
803 and its application. Gene 181:71–76.

804 43. Wei Z, Yang X, Yin S, Shen Q, Ran W, Xu Y. 2011. Efficacy of Bacillus-fortified organic fertiliser
805 in controlling bacterial wilt of tomato in the field. Applied Soil Ecology 48:152–159.

806 44. Guo J-H, Qi H-Y, Guo Y-H, Ge H-L, Gong L-Y, Zhang L-X, Sun P-H. 2004. Biocontrol of tomato
807 wilt by plant growth-promoting rhizobacteria. Biological Control 29:66–72.

808 45. Cardenas E, Wu W-M, Leigh MB, Carley J, Carroll S, Gentry T, Luo J, Watson D, Gu B,
809 Ginder-Vogel M, Kitanidis PK, Jardine PM, Zhou J, Criddle CS, Marsh TL, Tiedje JM. 2010.
810 Significant Association between Sulfate-Reducing Bacteria and Uranium-Reducing Microbial
811 Communities as Revealed by a Combined Massively Parallel Sequencing-Indicator Species
812 Approach. Appl Environ Microbiol 76:6778–6786.

813 46. Callahan BJ, McMurdie PJ, Rosen MJ, Han AW, Johnson AJA, Holmes SP. 2016. DADA2:
814 High-resolution sample inference from Illumina amplicon data. Nat Methods 13:581–583.

815 47. Caporaso JG, Kuczynski J, Stombaugh J, Bittinger K, Bushman FD, Costello EK, Fierer N, Peña
816 AG, Goodrich JK, Gordon JI, Huttley GA, Kelley ST, Knights D, Koenig JE, Ley RE, Lozupone CA,
817 McDonald D, Muegge BD, Pirrung M, Reeder J, Sevinsky JR, Turnbaugh PJ, Walters WA,
818 Widmann J, Yatsunenko T, Zaneveld J, Knight R. 2010. QIIME allows analysis of

819 high-throughput community sequencing data. Nat Methods 7:335–336.

820 48. Schönfeld J, Heuer H, Van Elsas JD, K. Smalla. 2003. Specific and Sensitive Detection of
821 *Ralstoniasolanacearum* in Soil on the Basis of PCR Amplification of *fliC* Fragments. Appl
822 Environ Microbiol 69:7248–7256.

823 49. Eden PA, Schmidt TM, Blakemore RP, Pace NR. 1991. Phylogenetic Analysis of Aquaspirillum
824 magnetotacticum Using Polymerase Chain Reaction-Amplified 16S rRNA-Specific DNA.
825 International Journal of Systematic Bacteriology 41:324–325.

826 50. Scheublin TR, Sanders IR, Keel C, Van Der Meer JR. 2010. Characterisation of microbial
827 communities colonising the hyphal surfaces of arbuscular mycorrhizal fungi. The ISME
828 Journal 4:752–763.

829 51. Eisenhauer N, Schulz W, Scheu S, Jousset A. 2013. Niche dimensionality links biodiversity
830 and invasibility of microbial communities. Functional Ecology 27:282–288.

831 52. Robinson MD, McCarthy DJ, Smyth GK. 2010. edgeR: a Bioconductor package for
832 differential expression analysis of digital gene expression data. Bioinformatics 26:139–140.

833 53. Klopfenstein DV, Zhang L, Pedersen BS, Ramírez F, Warwick Vesztrocy A, Naldi A, Mungall CJ,
834 Yunes JM, Botvinnik O, Weigel M, Dampier W, Dessimoz C, Flick P, Tang H. 2018. GOATOOLS:
835 A Python library for Gene Ontology analyses. Sci Rep 8:10872.

836 54. Wu J, Mao X, Cai T, Luo J, Wei L. 2006. KOBAS server: a web-based platform for automated
837 annotation and pathway identification. Nucleic Acids Research 34:W720–W724.

838 55. Liu C, Cui Y, Li X, Yao M. 2021. *microeco*: an R package for data mining in microbial
839 community ecology. FEMS Microbiology Ecology 97:fiaa255.

840 56. Dixon P. 2003. VEGAN, a package of R functions for community ecology. J Vegetation
841 Science 14:927–930.

842 57. Wang N, Zhang Y, Jiang G. 2024. LorMe: Lightening One-Code Resolving Microbial Ecology
843 Solution.

844 58. Gu Z, Eils R, Schlesner M. 2016. Complex heatmaps reveal patterns and correlations in
845 multidimensional genomic data. Bioinformatics 32:2847–2849.

846 59. Havenaar R, Bonnin-Marol S, Van Dokkum W, Petitet S, Schaafsma G. 1999. Inulin:
847 Fermentation and microbial ecology in the intestinal tract. Food Reviews International
848 15:109–120.

849 60. Oliveira RPDS, Perego P, De Oliveira MN, Converti A. 2012. Growth, organic acids profile and
850 sugar metabolism of Bifidobacterium lactis in co-culture with *Streptococcus thermophilus*:
851 The inulin effect. Food Research International 48:21–27.

852 61. Wang NR, Wiesmann CL, Melnyk RA, Hossain SS, Chi M-H, Martens K, Craven K, Haney CH.
853 2022. Commensal *Pseudomonas fluorescens* Strains Protect *Arabidopsis* from Closely
854 Related *Pseudomonas* Pathogens in a Colonization-Dependent Manner. mBio
855 13:e02892-21.

856 62. Stringlis IA, Yu K, Feussner K, De Jonge R, Van Bentum S, Van Verk MC, Berendsen RL,

857 Bakker PAHM, Feussner I, Pieterse CMJ. 2018. MYB72-dependent coumarin exudation
858 shapes root microbiome assembly to promote plant health. Proc Natl Acad Sci USA 115.

859 63. Feng H, Fu R, Luo J, Hou X, Gao K, Su L, Xu Y, Miao Y, Liu Y, Xu Z, Zhang N, Shen Q, Xun W,
860 Zhang R. 2023. Listening to plant's Esperanto via root exudates: reprogramming the
861 functional expression of plant growth-promoting rhizobacteria. New Phytologist
862 239:2307–2319.

863 64. Ling N, Raza W, Ma J, Huang Q, Shen Q. 2011. Identification and role of organic acids in
864 watermelon root exudates for recruiting *Paenibacillus polymyxa* SQR-21 in the rhizosphere.
865 European Journal of Soil Biology 47:374–379.

866 65. Naloka K, Kuntaveesuk A, Muangchinda C, Chavanich S, Viyakarn V, Chen B, Pinyakong O.
867 2024. *Pseudomonas* and *Pseudarthrobacter* are the key players in synergistic phenanthrene
868 biodegradation at low temperatures. Sci Rep 14:11976.

869 66. Samal S, Singh D, Upadhyay RS, Lokesh Babu P, Geat N. 2024. Hydrolytic genes of
870 antagonistic rhizobacteria strains on Fusarium udum causing wilt disease in pigeonpea. J
871 Plant Pathol https://doi.org/10.1007/s42161-024-01641-z.

872 67. Ghasemi Z, Ghaderian SM, Rodríguez-Garrido B, Prieto-Fernández Á, Kidd PS. 2018. Plant
873 species-specificity and effects of bioinoculants and fertilization on plant performance for
874 nickel phytomining. Plant Soil 425:265–285.

875 68. Adamo I, Acin-Albiac M, Röttjers S, De Prado DR, Benito BM, Zamora J, Godara R,
876 García-Jiménez B, Jiang-Rempel P, Cline LC, Acedo A. 2024. Short impact on soil microbiome

877 of a *Bacillus amyloliquefaciens* QST713 based product that correlates with higher potato
878 yield across USA. Front Plant Sci 15:1332840.

879 69. Laird M, Piccoli D, Weselowski B, McDowell T, Renaud J, MacDonald J, Yuan Z-C. 2020.
880 Surfactin-producing Bacillus velezensis 1B-23 and *Bacillus* sp. 1D-12 protect tomato against
881 bacterial canker caused by Clavibacter michiganensis subsp. michiganensis. J Plant Pathol
882 102:451–458.

883 70. Huang R, Li GQ, Zhang J, Yang L, Che HJ, Jiang DH, Huang HC. 2011. Control of Postharvest
884 Botrytis Fruit Rot of Strawberry by Volatile Organic Compounds of *Candida intermedia*.
885 Phytopathology® 101:859–869.

886 71. Zhao X, Zhou J, Tian R, Liu Y. 2022. Microbial volatile organic compounds: Antifungal
887 mechanisms, applications, and challenges. Front Microbiol 13:922450.

888 72. Zhou X, Zhang J, Shi J, Khashi U Rahman M, Liu H, Wei Z, Wu F, Dini-Andreote F. 2024.
889 Volatile-mediated interspecific plant interaction promotes root colonization by beneficial
890 bacteria via induced shifts in root exudation. Microbiome 12:207.

891